Noncovalent Polymer-Gatekeeper in Mesoporous Silica Nanoparticles as a Targeted Drug Delivery Platform

L. Palanikumar, Eun Seong Choi, Jae Yeong Cheon, Sang Hoon Joo, and Ja-Hyoung Ryu**

Selective targeting of tumor cells and release of drug molecules inside the tumor microenvironment can reduce the adverse side effects of traditional chemotherapeutics because of the lower dosages required. This can be achieved by using stimuli-responsive targeted drug delivery systems. In the present work, a robust and simple one-pot route is developed to synthesize polymer-gatekeeper mesoporous silica nanoparticles by noncovalent capping of the pores of drug-loaded nanocontainers with disulfide cross-linkable polymers. The method offers very high loading efficiency because chemical modification of the mesoporous nanoparticles is not required; thus, the large empty pore volume of pristine mesoporous silica nanoparticles is entirely available to encapsulate drug molecules. Furthermore, the polymer shell can be easily decorated with a targeting ligand for selective delivery to specific cancer cells by subsequent addition of the thiol-containing ligand molecule. The drug molecules loaded in the nanocontainers can be released by the degradation of the polymer shell in the intracellular reducing microenvironment, which consequentially induces cell death.

1. Introduction

Ideal nanocarriers should maintain highly stable encapsulation until they reach the target tumor cell during blood circulation, yet afford efficient release at the target tumor tissue or inside the tumor cell.[1] Stimulus-responsive release of therapeutic molecules from delivery vehicles is one of the most promising strategies in nanomedicine and pharmaceutical sciences.[2] To prevent undesirable off-target release of drug molecules as well as to ensure release only in the vicinity of the target, the vehicle should provide triggered, controlled release in response to specific stimuli.[3] Among the variety of stimulus-responsive systems including polymeric micelles, polymersomes, liposomes, dendrimers, metal nanoparticles, and nanogels, mesoporous silica nanoparticles (MSNs) have attracted considerable attention for biomedical applications since MSNs have numerous, well-defined pores that hold the drug molecule inside, and can be modified with several stimulus-responsive gatekeepers to release the drug only in the presence of specific triggers.[4]

To date, various synthetic strategies to implement the gatekeeper concept have been developed by covalent conjugations with silane chemistry using abundant silanol (Si–OH) groups on the surface.[5] Gatekeepers consisting of stimuli-sensitive functional groups or nanoparticles can block the pore entrance, stably retaining the drug molecules inside the pore until the cargo is released by external stimuli such as pH, temperature, light, competitive binding, or enzymes.[6] However, the installation of functional groups onto the surface of MSNs requires complicated synthetic steps. Surface modification of the MSNs before drug loading limits loading efficiency due to the reduced pore volume available for guest encapsulation. Several steps of the post functionalization of drug-loaded MSNs result in the leakage of the cargo.[7] Additionally, targeting ligand installation onto gatekeeper MSNs requires further chemical modification, limiting the robustness and versatility of ligand functionalization.

Here, we report a simple and robust method for one-pot synthesis of ligand-decorated, stimulus-responsive MSNs that can encapsulate doxorubicin hydrochloride (Dox) or cisplatin with very high drug loading (44 and 33 wt%, respectively), without multiple chemical modifications (**Figure 1**). The pores of MSNs filled with the drug molecules are noncovalently end-capped with a biocompatible self-crosslinkable random copolymer containing pyridine disulfide hydrochloride (PDS) and polyethylene glycol (PEG) as side chains. PEG on the surface of MSNs provides water solubility and prevents nonspecific interactions with biomacromolecules.[8] PDS facilitates wrapping of the MSNs surface through the weak electrostatic interaction between the MSNs and the polymer, and subsequently, through crosslinking by disulfide exchange reactions within the polymer shell of the MSNs.[9] In order to target cancer cells, cyclic (Arg-Gly-Asp-D-Phe-Cys) (cRGDfC), a well-known ligand for cell-surface integrins on tumor endothelium, can be simply attached to the surface of the MSNs by disulfide bond

Dr. L. Palanikumar, E. S. Choi, J. Y. Cheon, Prof. S. H. Joo, Prof. J.-H. Ryu
Department of Chemistry
School of Natural Sciences
Ulsan National Institute of Science and Technology (UNIST)
Ulsan 689–798, South Korea
E-mail: shjoo@unist.ac.kr; jhryu@unist.ac.kr
Prof. S. H. Joo
School of Energy and Chemical Engineering
Ulsan National Institute of Science and Technology (UNIST)
Ulsan 689–798, South Korea

DOI: 10.1002/adfm.201402755

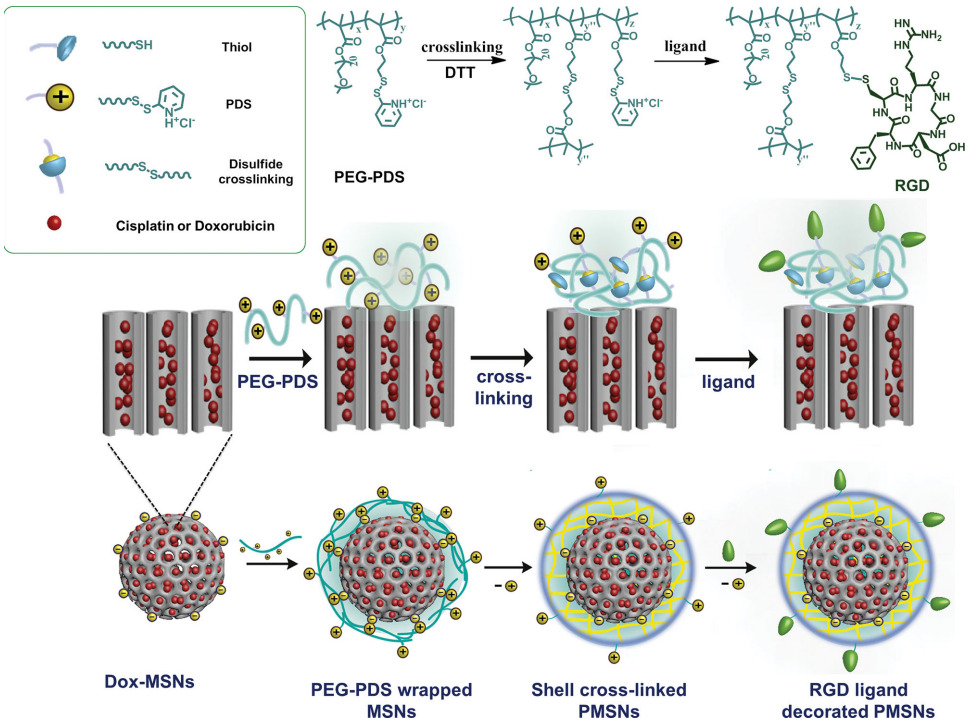

Figure 1. Schematic representation of one-pot synthetic procedure for polymer-gatekeeper MSNs with stimuli responsive polymer (PEG-PDS) and decorating the surface with targeting ligand (cRGDfC).

formation.[10] Note that PDS has multiple roles as a sacrificial functional group. It acts temporarily as a positive charge to wrap the negatively charged MSNs, as a crosslinker to stabilize the shell of polymer-MSNs, and as a functional group on the surface to attach the targeting ligand. We demonstrate the versatility and robustness of these multifunctional MSNs by showing the following: (1) Hydrophilic drug molecules can be encapsulated at high doses, since the MSNs are not chemically modified, thereby providing maximum pore volume. (2) The polymer-gatekeepers can be easily installed by self-crosslinking to the polymer shell which coats the MSNs through weak electrostatic interactions. (3) The drug molecules can be released in response to an intracellular biological stimulus and the release kinetics can be controlled by the crosslinking density of the polymer-gatekeeper. (4) The surface of polymer-capped MSNs can be functionalized with a target ligand that undergoes facilitated cell internalization by receptor-mediated uptake. The drug is released by intracellular reducing agents such as glutathione (GSH) to effectively kill the cancer cells.[11]

2. Results and Discussion

2.1. Preparation of Polymer-Gatekeeper MSNs (PMSNs) with High Drug Loading

Ordered MCM-41 type MSNs were prepared by the Stöber process with cetyltrimethylammonium bromide (CTAB) as a template via base-catalyzed co-condensation of silicates.[12] MSNs were characterized by X-ray diffraction (XRD), transmission electron microscopy (TEM), and nitrogen adsorption analysis. A well-ordered hexagonal mesostructure was obtained, as observed from well-defined three diffraction peaks in the XRD patterns (Figure S1, Supporting Information). Nitrogen adsorption–desorption isotherm measurements showed that the MSNs have a large Brunauer-Emmett-Teller (BET) surface area of 789 m^2 g^{-1}, with a total pore volume of 0.79 cm^3 g^{-1}, and a pore size of 2.4 nm. We hypothesized that unmodified pristine MSNs would provide a larger volume for drug encapsulation than chemically modified MSNs for the conventional gatekeeper strategy that gives less than 10 wt% loading efficiency.[13] Supramolecular nanovalves and nanogates on the surface of MSNs are a groundbreaking concept for controlled delivery carriers.[13] These systems, however, require surface functionalization of the MSNs with various chemical modifications, leading to altered physicochemical parameters. These reactions might decrease the volume of the pores to limit encapsulation of large mass molecules.[14] Recent reports have demonstrated that conservation of high pore volume is needed to achieve high drug payloads and the degree of the surface modification should be optimized to preserve the pore volume.[8c] In our system, we use pristine MSNs to encapsulate the drug molecules, without modifying the surface of the MSNs (Figure 1). Therefore, we can utilize maximum capacity for loading drug molecules inside the pores. The loading capacity and entrapment efficiency are determined by varying the ratio of drug to nanoparticles. We hypothesized that increasing the feeding amount of drug would increase the loading (**Table 1**). Indeed, the pristine MSNs showed a large loading content of 44 wt%, with entrapment efficiency of 73%, as the feeding concentration of Dox drug molecules was increased. This loading efficiency is significantly high because of the large unmodified pore volume.

Table 1. Drug loading and entrapment efficiency by varying the mass ratio of drug to MSNs.

Sample	Dox [mg]	MSN [mg]	Loading efficiency	Entrapment efficiency [%]
MSN-1	0.9	5.0	10 wt% (0.172 μmol mg^{-1})	62
MSN-2	2.1	5.0	19 wt% (0.328 μmol mg^{-1})	56
MSN-3	2.9	5.0	24 wt% (0.414 μmol mg^{-1})	54
MSN-4	4.4	5.0	39 wt% (0.672 μmol mg^{-1})	73
MSN-5	5.4	5.0	44 wt% (0.759 μmol mg^{-1})	73

To stably hold the drug molecules inside the pores, we installed the polymer-gatekeeper on the surface of Dox-containing MSNs by using simple electrostatic interactions between the negatively charged MSNs and a positively charged copolymer, followed by crosslinking reaction of the polymer shell. We used in situ, one-pot functionalization to avoid the leakage of hydrophilic drug during the preparation process of the polymer-gatekeeper. The random copolymer was prepared by reversible addition-fragmentation chain transfer polymerization (Scheme S1 and Figure S2, Supporting Information). Polymer-wrapped MSNs were prepared by incubation of MSNs and PEG-PDS polymer in water. To determine the optimal amount of polymer required to stably wrap the MSNs, we measured the remaining amount of polymer in the supernatant after centrifugation of MSNs that had been incubated with the copolymer. When the polymer concentration was varied from 2.5 to 10 mg mL^{-1} with 5 mg of MSNs, we found that the polymer wrapping was stable over certain concentrations (**Figure 2**a and Figure S3, Supporting Information). We investigated the drug release profile to confirm that the polymer-capping efficiently blocked the leakage of drug molecules. As shown in Figure 2b, at low concentrations of the polymer, 2.5 or 5 mg mL^{-1}, burst release of the drug occurred within 1 h, indicating that these amounts of polymer are insufficient to prevent the leakage of drug molecules from the pore of the MSNs. In contrast, at a polymer concentration of 10 mg mL^{-1}, the release of the drug molecules was slow. Crosslinking of the polymer shell effectively blocked the pore, inhibiting leakage of drug molecules. Based on these observations, in further experiments, we used a 2:1 ratio (w/w) of the polymer to MSNs in order to provide a sufficient amount of polymer.

Polymer-wrapped MSNs might be useful as a zero-order drug release system, since the drug molecules are continuously released in the absence of a stimulus because the electrostatic interaction between the polymer and MSNs would weaken in a physiological environment containing many charged components such as serum proteins and red blood cells.[14] However, to avoid the severe side effects that would occur with premature drug release from the targeted drug delivery system, the drug molecules should be stably located inside until they reach the target diseased cell.[15] To accomplish this, the resulting polymer shell on the MSNs surface was crosslinked by disulfide formation between the polymer chains. Addition of a certain amount of dithiothreitol (DTT) would cause the cleavage of a well-defined percentage of PDS groups to the corresponding free thiol groups. The free thiols could then react with remaining PDS functional groups to form disulfide bonds (Figure 1). This

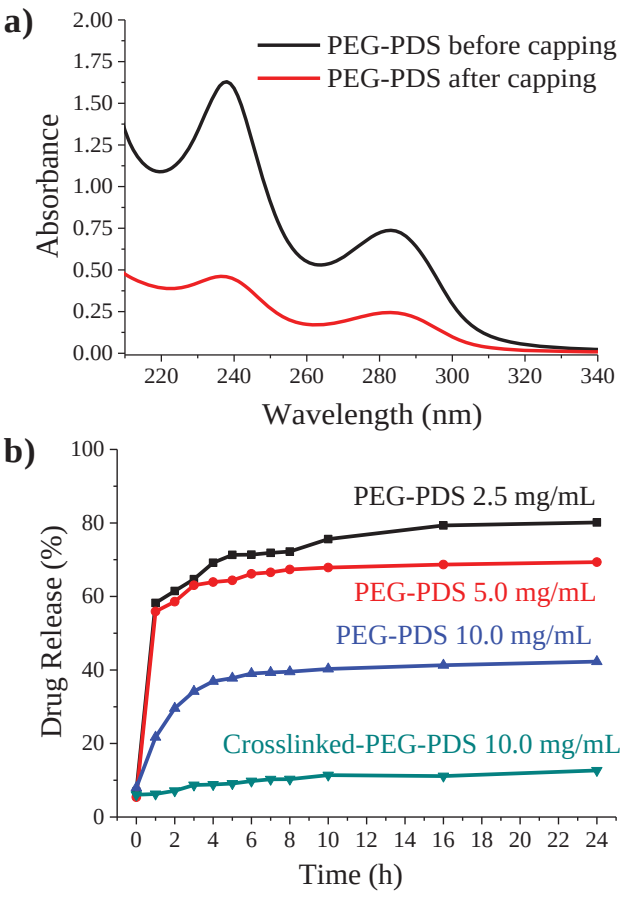

Figure 2. a) UV–vis spectra of the supernatant for PEG-PDS solution before and after capping the MSNs (10 mg mL^{-1} copolymer solution). b) Drug release profiles for 2.5, 5.0, and 10.0 mg mL^{-1} copolymer wrapped MSNs and polymer shell cross-linked PMSNs.

mild and fast intra/intermolecular disulfide exchange reaction occurs in the polymer layer, resulting in a crosslinked polymer shell that very stably holds the drug cargo. Also, the reaction is simple and does not require the use of metal-containing catalysts or solvents that may cause toxicity.[16] We hypothesized that varying the amount of DTT would determine the degree of cross-linking. The byproduct of this reaction, pyridothione, was monitored by UV–vis spectroscopy and the crosslinking density was calculated (**Figure 3**a). Since wrapping and crosslinking occur under very mild conditions, the entrapped drug molecules are stably retained in the pore during the formation of the polymer-gatekeeper. The loading efficiency was found to be around 32–39 wt%, which is very high for a drug delivery system. On the basis of pyridothione release, we found that the mol% of PDS consumed ranged between 19 and 83 mol% after the addition of varying amounts of DTT from 12 to 60 mol% (**Table 2**).

The prepared PMSNs were characterized by dynamic light scattering (DLS), zeta-potential measurements, and TEM. As shown in Figure 3b, the size of the MSNs was 124 nm and the PMSNs size increased to 160 nm. The surface charge of the MSNs was highly negative (–54 mV), but became almost neutral (–1 mV) after the introduction of the PEG-PDS copolymer

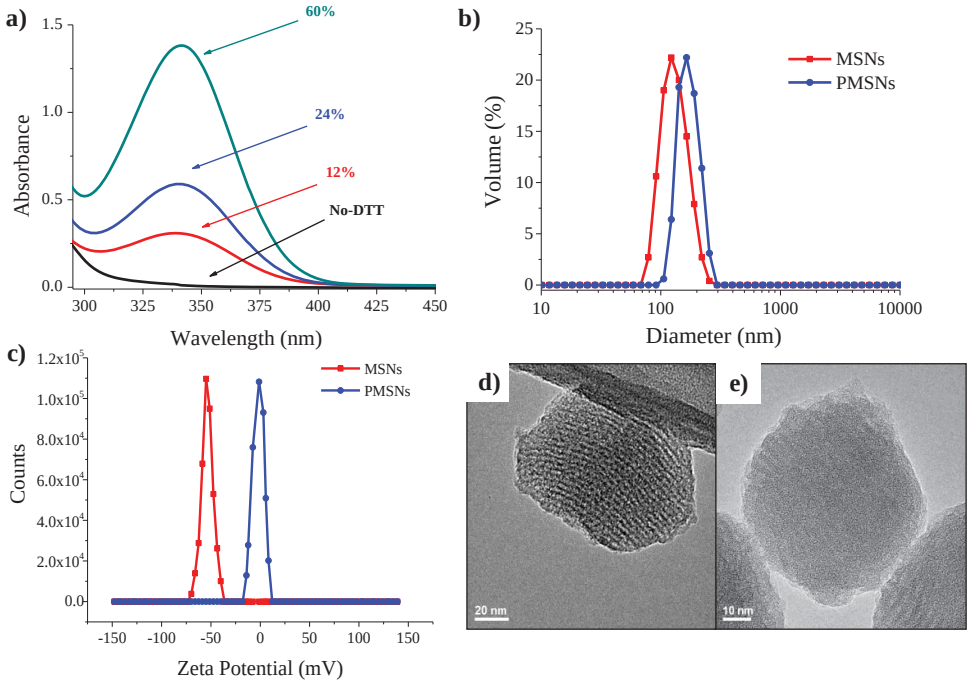

Figure 3. a) UV–vis spectra of byproduct pyridiothione by the addition of partial amount of DTT against mol% of PDS groups in PEG-PDS. b) Size distribution and c) zeta potential analysis for MSNs and PMSNs. d,e) TEM images of MSNs and PMSNs.

on the surface of the drug-loaded MSNs (Figure 3c). Considering that the surface charges of the nanoparticles have a serious impact on cellular internalization,[17] the neutral PEG outer layers of the resulting PMSNs can be favorable for protein resistance[18] and increase the prolong circulation time. The TEM images of MSNs and PMSNs illustrated the change in the porous nature after polymer capping on the surface of the MSNs (Figure 3d,e). While MSNs showed clear porous nature, no pores were visible on the PMSNs after polymer wrapping.[19] The PMSNs had shown a good colloidal stability in aqueous suspension and culture medium ranging around ≈190 nm and ≈200 nm, respectively (Figure S4, Supporting Information). At pH 7.4 (phosphate buffered saline) and in serum containing RPMI1640 cell culture medium, it ranged at ≈190 nm and ≈200 nm, respectively. Similarly, it was ≈180 nm in pH 5.5 sodium acetate buffer solution. No adverse change in size and aggregation has been noted until we analyzed for 72 h, indicative of the long term colloidal stability in biologically relevant fluids.

Table 2. Estimated crosslinking density of polymer shell based on mol% of PDS consumed, drug loading, and entrapment efficiency of Dox loaded PEG-PDS capped MSNs.

DTT [mol% against PDS group]	Cross-linking density[a] (mol% of PDS consumed)	Drug loading (entrapment efficiency)
12	19	32 wt%, 0.552 μmol mg^{-1} (53%)
24	36	33 wt%, 0.569 μmol mg^{-1} (56%)
60	83	39 wt%, 0.672 μmol mg^{-1} (73%)

[a]Based upon mol% of PDS cleaved, crosslinking density was theoretically calculated by assuming that the formation of a single, cross-linking disulfide bond would require cleavage of two PDS units and produce two pyridiothione molecules. The known molar excitation coefficient of pyridiothione was 8.08×10^3 M^{-1} cm^{-1} at 343 nm.

2.2. Triggered Drug Release Profile

As described above, PMSNs showed a very stable encapsulation without any leakage of drug molecules over 24 h. Since the polymer crosslinking is formed by disulfide bonds, the polymer shell can be degraded by reducing agents and the drug can be released by opening the gate in response to the external stimuli. To show the triggered drug release, we investigated the release profile of Dox from polymer-gatekeeper nanocarriers in phosphate buffered saline (pH 7.4) by using a fluorometer to measure the emission increase when Dox is released from PMSNs. We introduced varying GSH concentrations (1×10^{-3}, 5×10^{-3}, and 10×10^{-3} M) to the aqueous suspension of Dox loaded nanoparticles after 4 h. As shown in **Figure 4**a, increasing concentration of the reducing agent results in an accelerated release of guest molecules by the reduction of disulfide stalk moieties.[20] Cancer cells are rich in GSH, which can obviously cleave the disulfide linkage and trigger drug release inside the cell.[17] In addition, the drug release kinetics could be controlled depending on the crosslinking density of the polymer shell on the MSNs. As shown in Figure 4b, 19%-crosslinked MSNs showed fast release upon addition of 5×10^{-3} M of GSH at 4 h, 83%-crosslinked MSNs showed sustained release, and 36%-crosslinked sample showed moderate release. This indicates that the release rate can be fine-tuned in a controlled manner for specific drug delivery systems.

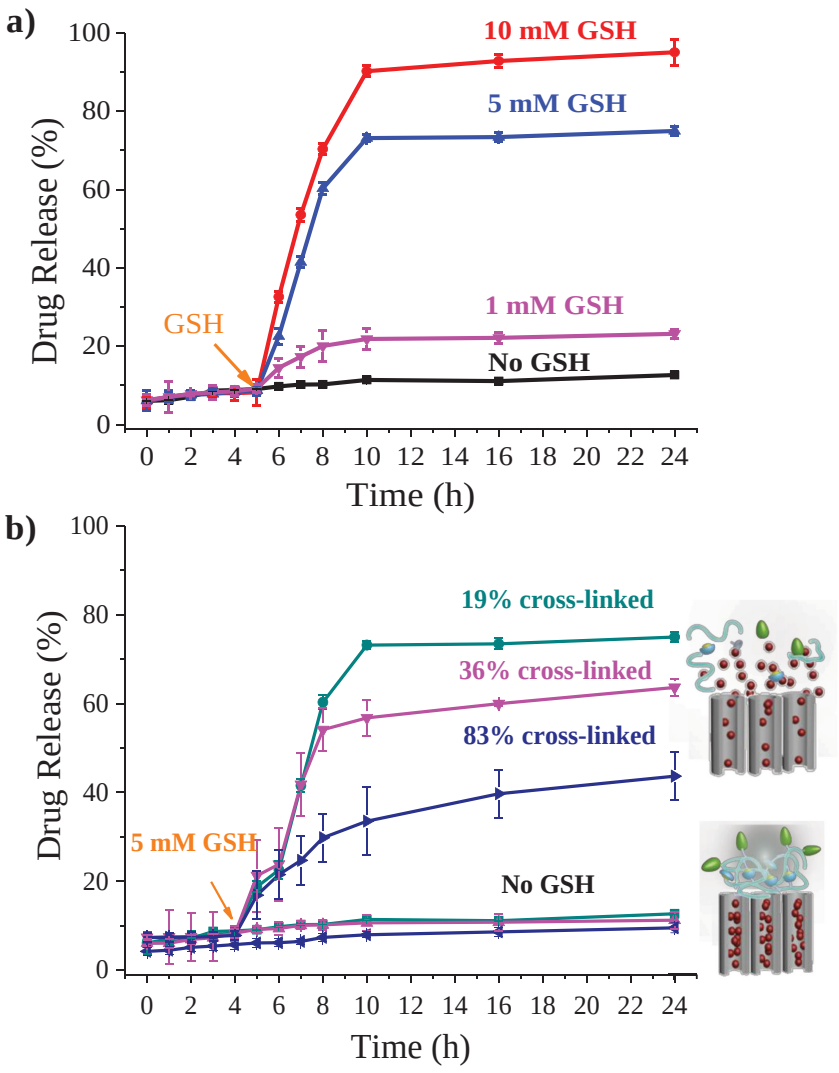

Figure 4. On-demand/triggered release profile analysis by the addition of a) 1×10^{-3}, 5×10^{-3}, and 10×10^{-3} M GSH concentrations at 4 h to PMSNs and b) 5×10^{-3} M GSH to PMSNs with different cross-linking densities.

2.3. Pore Morphology Dependency of Drug Release Profile

Considering that the pore can be blocked through the crosslinked polymer shell, we envision that the polymer-gatekeeper strategy can be applied to other types of porous structures. We prepared raspberry-type MSNs (rMSNs) by a previously reported method[21] and characterized by XRD, TEM, and nitrogen adsorption analysis (Figure S5, Supporting Information). A disordered mesoporous structure was obtained, compared to MCM-41, as observed from the XRD pattern and TEM image. We hypothesized that pore morphology can affect drug encapsulation and drug release profile as part of the polymer-gatekeeper strategy. To investigate this, we prepared Dox-rMSNs and installed polymer-gatekeeper (PrMSNs) by using the same method as used above with PMSNs. The PrMSNs were characterized by DLS, zeta-potential measurements, and TEM as shown in **Figure 5**. The surface charges of the rMSNs were highly negative (–44 mV), becoming almost neutral after coating (–2 mV). Similar to the case of PMSNs, we optimized the drug loading efficiency, which reached a maximum of 28% (Table S2, Supporting Information). We investigated the drug release profile by varying the shell crosslinking density (19%, 36%, and 83%) in phosphate-buffered saline (pH 7.4). While PMSNs stably hold their cargo even at low crosslinking density (Figure 4b), PrMSNs require high crosslinking density to avoid drug leakage, indicating that the varied porous nature and morphology influence the release profile (**Figure 6**a). We analyzed the triggered release profile by adding increasing concentrations of GSH (1×10^{-3}, 5×10^{-3}, and 10×10^{-3} M) in the 83% shell crosslinked Dox-loaded PrMSNs. As shown in Figure 6b, the concentration of the reducing agent influenced the release profile. This indicates that the polymer-gatekeeper strategy can be applied to particles that vary in their porous nature, and that the shell crosslinking density influences the release profile of a drug delivery system.

2.4. Ligand Decoration on PMSNs (RGD-PMSNs) and Targeted Delivery

For targeted delivery systems, the surface of PMSNs can be decorated with a cysteine-containing ligand by a disulfide exchange reaction with the remaining surface PDS units. The cysteine-containing peptide ligand cRGDfC was added to the reaction mixture after crosslinking to modify the surface of the nanocarriers. The attachment of the ligand was evaluated by further observation of pyridothione adsorption at 343 nm (**Figure 7**a). About 3.62×10^{-8} moles of ligand was decorated on the surface for PMSNs nanocarriers. We tested the cell viability of KB cells (human nasopharyngeal carcinoma cell lines) in the presence of MSNs and PMSNs without the drug to show the biocompatibility of the nanocarriers. Pristine MSNs or PMSNs were added to the cells at different concentrations and cell viability was analyzed by the Alamar Blue assay at varying time points (Figure S6, Supporting Information). We observed that pristine MSNs and PMSNs did not show toxicity up to a reasonably high concentration of 2 mg mL^{-1}, suggesting that PMSNs are nontoxic and biocompatible for use as a drug delivery system. Importantly, 0.25–2 μg mL^{-1} Dox in cRGDfC ligand-decorated PMSNs (RGD-PMSNs) showed significantly higher toxicity compared to nonligand-decorated PMSNs (Figure 7b). This suggests that RGD-PMSNs could be rapidly internalized by ligand-mediated endocytosis and release the drug molecule to kill the cancer cells.[22] Internalization of Dox-loaded PMSNs and RGD-PMSNs was further confirmed by confocal fluorescence microscopy (Figure 7c and Figure S7, Supporting Information).

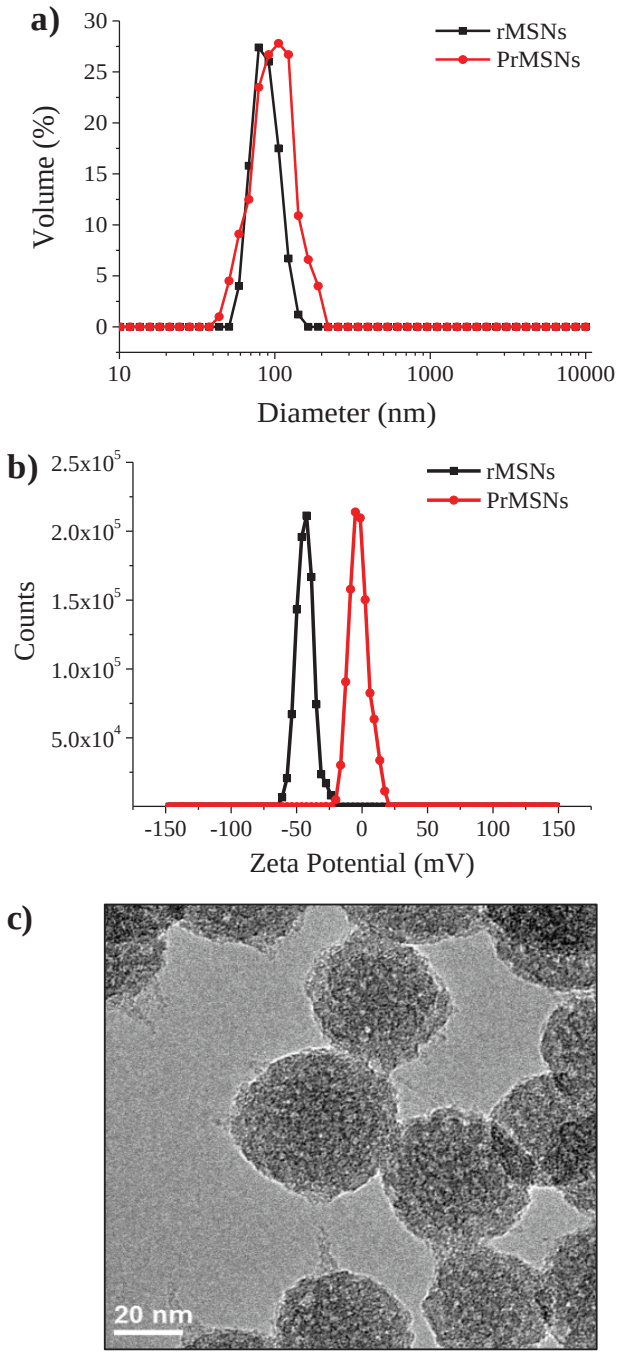

Figure 5. a) Size distribution and b) zeta potential analysis for rMSNs and PrMSNs. c) A TEM image of PrMSNs.

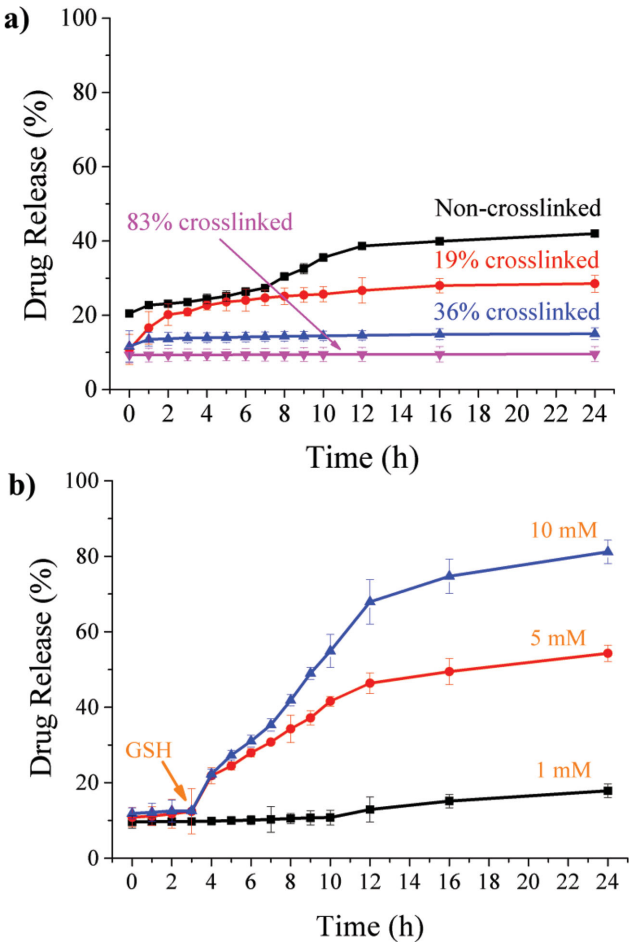

Figure 6. a) Release profile analysis depending on crosslinking density of PrMSNs. b) On-demand/triggered release profiles by the addition of 1×10^{-3}, 5×10^{-3}, and 10×10^{-3} M GSH concentrations at 4 h to the 83% shell cross-linked PrMSNs.

The red color from Dox was distributed in the cells, which indicated that a large quantity of the ligand-decorated nanoparticle-loaded drug was internalized into the cells within 30 min. In contrast, nonligand decorated nanoparticles did not show any internalization in the same period. This suggests that efficient uptake occurs by ligand-mediated endocytosis. To quantitatively measure the uptake of Dox-loaded PMSNs in the presence or absence of ligand, KB cells were analyzed by flow cytometry. As shown in Figure 7d, significant differences were noted between the cellular uptake of ligand-decorated and nondecorated nanocarriers. These results confirm that RGD-PMSNs are selective for cancerous cells that overexpress cell surface integrin. In addition, nonligand decorated PMSNs did not produce an obvious inhibitory effect on the cell viability of tumor cells. These results indicate that the existence of the cRGDfC motif on the surface enhanced the cellular uptake and that drugs are released because of the cleavage of polymer capping on the surface, in response to intracellular stimuli.[23]

2.5. Cisplatin-Loaded PMSNs

To test whether this polymer-gatekeeper can be applied as a versatile delivery platform for hydrophilic drugs, we investigated the polymer-gatekeeper strategy using cisplatin, as another hydrophilic drug, in the MCM-41 type MSNs. We loaded cisplatin in the MSNs, wrapped the surface with PEG-PDS, and varied the shell crosslinking density (19%, 36%, and 83%). The drug loading efficiency of cisplatin was 33%. To check its stable encapsulation, we analyzed the cisplatin release profile in phosphate-buffered saline (pH 7.4) by high-performance

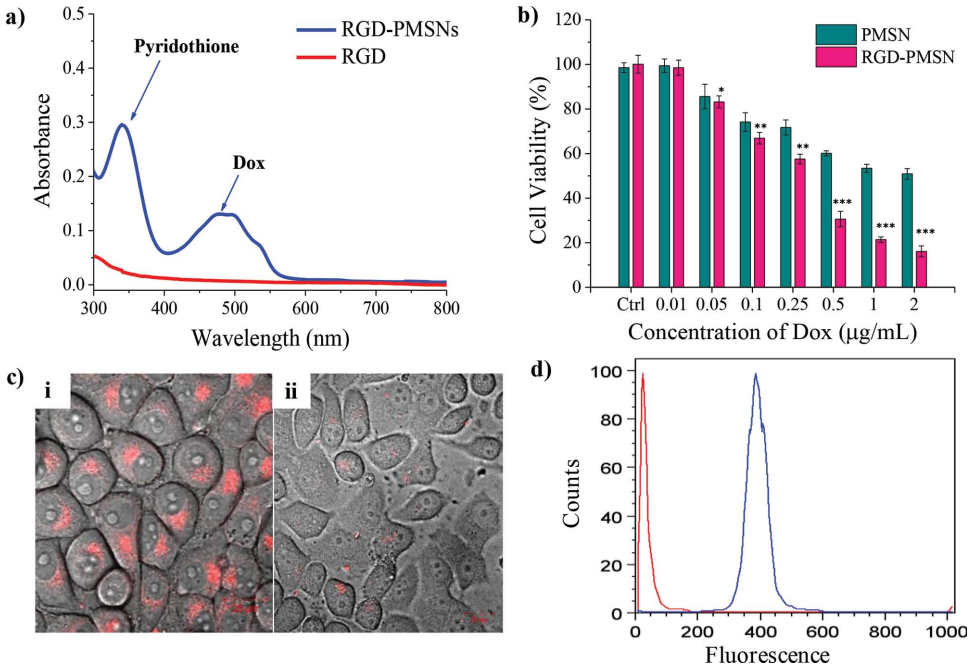

Figure 7. a) UV–vis spectra for RGD ligand decoration in PMSNs. b) Cell viability analysis for Dox-loaded PMSNs and RGD-PMSNs. c) CLSM images for the cellular uptake of (i) RGD-PMSNs and (ii) PMSNs at 30 min. d) Flow-cytometry analysis for cellular uptake investigation in KB cells at 3 h (red: PMSNs; blue: RGD-PMSNs). *P < 0.05; **P < 0.01, and ***P < 0.001 compared to control, analyzed by students t-test.

liquid chromatography. Similar to Dox-loaded PMSNs, shell crosslinking efficiently blocked cisplatin leakage (**Figure 8**a). Triggered release kinetics was investigated by the addition of 5×10^{-3} M GSH to the 19%, 36%, and 83% shell-crosslinked cisplatin-loaded PMSNs, as shown in Figure 8b. Varying crosslinking density alters the release profile. These results indicate that the polymer-gatekeeper concept can work as a versatile hydrophilic drug delivery system with high drug loading.

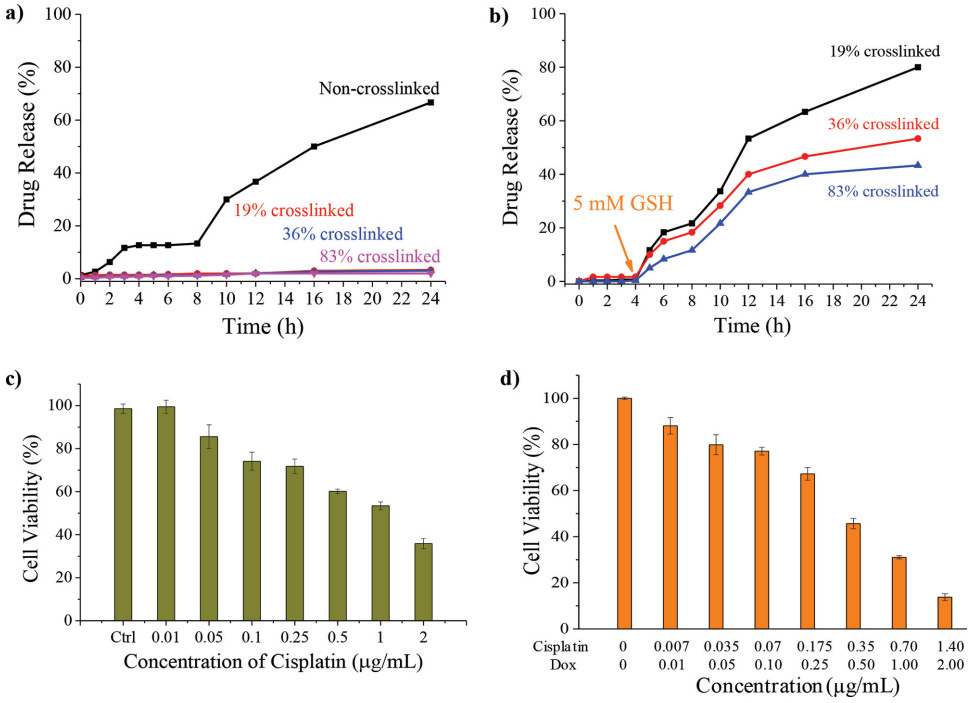

Figure 8. Drug release profiles for a) cisplatin-loaded PMSNs depending on the crosslinking density and b) triggered release of cisplatin upon addition of 5×10^{-3} M GSH. c) Cytotoxicity analysis for cisplatin-loaded PMSNs at 48 h in KB cells. d) Cytotoxicity analysis for dual drug loaded PMSNs (cisplatin and Dox) at 48 h in KB cells.

In vitro cytotoxicity analysis of KB cells with cisplatin-loaded PMSNs showed a varied cytotoxic response, due to drug release upon opening the polymer-gatekeepers in response to intracellular GSH (Figure 8c).

In recent years, combination therapy with nanoparticles has become an important approach to overcome drug resistance and facilitate controlled dosing.[24,25] We tried dual drug delivery using the polymer-gatekeeper strategy by varying the time for loading the hydrophilic drugs, namely, cisplatin and Dox. The drug loading efficiency was 14% for cisplatin and 25% for Dox (Table S3, Supporting Information). Cytotoxicity analysis with KB cells showed that higher toxicity was observed for dual drug-loaded nanoparticles (Figure 8d) than for treatment with a single drug. Since Dox induces the cytotoxic response by intercalating with DNA, while cisplatin crosslinks with DNA and induces apoptosis,[26] this simple dual drug delivery strategy using polymer-gatekeepers can be applied to multidrug resistance systems and combination therapies.

3. Conclusion

In summary, we have designed and fabricated a novel type of stimulus-responsive polymer-gatekeeper drug delivery system for tumor targeting. Drug molecules could be effectively loaded into MSNs at a very high loading efficiency, and stably located inside the pore by simple, noncovalent blocking of pores with a stimulus-responsive polymer. Furthermore, an integrin-targeting ligand could be simply installed on the surface by disulfide chemistry. The addition of varying amounts of the intracellular small peptide GSH induced the cleavage of the wrapped polymer in a concentration-dependent manner, resulting in a controlled and on-demand release profile. Moreover, cell viability, microscopy, and flow-cytometry analyses consistently confirmed that the internalization of these carriers is target specific in nature. This strategy reduces chemical modifications and allows the particles to be selectively recognized by diseased cells. We believe that the development of such a biocompatible system with noncovalent polymer-gatekeepers in the mesoporous carriers provides a versatile method for hydrophilic drug delivery and opens wide range of research opportunities for research on biomaterials.

Supporting Information

Supporting Information is available from the Wiley Online Library or from the author.

Acknowledgements

This work was supported by a National Research Foundation of Korea (NRF) grant funded by the Korean Government (Ministry of Education, Science and Technology, Grant No. NRF-2011–35B-C00024) and Ulsan National Institute of Science and Technology (2013 Future Challenge Research Fund, 1.130038). We thank S. Shin for help with the polymer synthesis.

Received: August 12, 2014
Revised: December 4, 2014
Published online: December 23, 2014

[1] a) Q. Zhang, X. Wang, P. Z. Li, K. T. Nguyen, X. J. Wang, Z. Luo, H. Zhang, N. S. Tan, Y. Zhao, *Adv. Funct. Mater.* **2014**, *24*, 2450; b) S. Tang, X. Huang, X. Chen, N. Zheng, *Adv. Funct. Mater.* **2010**, *20*, 2442; c) W. Zhao, H. Chen, Y. Li, L. Li, M. Lang, J. Shi, *Adv. Funct. Mater.* **2008**, *18*, 2780; d) C. H. Lee, L. W. Lo, C. Y. Mou, C. S. Yang, *Adv. Funct. Mater.* **2008**, *18*, 3283; e) H. Wu, S. Zhang, J. Zhang, G. Liu, J. Shi, L. Zhang, X. Cui, M. Ruan, Q. He, W. Bu, *Adv. Funct. Mater.* **2011**, *21*, 1850; f) D. Tarn, D. P. Ferris, J. C. Barnes, M. W. Ambrogio, J. F. Stoddart, J. I. Zink, *Nanoscale* **2014**, *6*, 3335; g) X. Ma, C. Teh, Q. Zhang, P. Borah, C. Choong, V. Korzh, Y. Zhao, *Antioxidant. Redox. Signal* **2014**, *21*, 707.

[2] a) A. Bernardos, L. Mondragon, E. Aznar, M. D. Marcos, R. Martinez-Manesz, F. Sancenon, J. Soto, J. M. Barat, E. Perez-Paya, C. Guillem, P. Amoros, *ACS Nano* **2010**, *11*, 6353; b) Y. Piao, A. Burns, J. Kim, U. Wiesner, T. Hyeon, *Adv. Funct. Mater.* **2008**, *18*, 3745; c) Y. Chen, H. Chen, S. Zhang, F. Chen, L. Zhang, J. Zhang, M. Zhu, H. Wu, L. Guo, J. Feng, J. Shi, *Adv. Funct. Mater.* **2011**, *21*, 270; d) Y. Itoh, M. Matsusaki, T. Kida, M. Akashi, *Biomacromolecules* **2006**, *7*, 2715; e) L. Jia, D. Cui, J. Bignon, A. D. Cicco, J. Wdzieczak-Bakala, J. Liu, M. H. Li, *Biomacromolecules* **2014**, *15*, 2206; f) Z. Luo, Y. Hu, K. Cai, X. Ding, Q. Zhang, M. Li, X. Ma, B. Zhang, Y. Zeng, P. Li, J. Li, J. Liu, Y. Zhao, *Biomaterials* **2014**, *35*, 7951; g) A. Jana, K. T. Nguyen, X. Li, P. Zhu, N. S. Tan, H. Agren, Y. Zhao, *ACS Nano* **2014**, *8*, 5939.

[3] a) C. Acosta, E. Pérez-Esteve, C. A. Fuenmayor, S. Benedetti, M. S. Cosio, J. Soto, F. Sancenón, S. Mannino, J. Barat, M. D. Marcos, R. Martínez-Manez, *ACS Appl. Mater. Interfaces* **2014**, *6*, 6453; b) H. Li, J. Z. Zhang, Q. Tang, M. Du, J. Hu, D. Yang, *Mater. Sci. Eng. C* **2013**, *33*, 3426; c) H. Wen, J. Guo, B. Chang, W. Yang, *Eur. J. Pharma. Biopharm.* **2013**, *84*, 91; d) C. Wang, Z. Li, D. Cao, Y. Zhao, J. W. Gaines, O. A. Bozdemir, M. W. Ambrogio, M. Frasconi, Y. Y. Botros, J. I. Zink, J. F. Stoddart, *Angew. Chem. Int. Ed.* **2012**, *51*, 5460; e) X. Ma, Y. Zhao, K. W. Ng, Y. Zhao, *Chem. Eur. J.* **2013**, *19*, 15593.

[4] a) N. Singh, A. Karambelkar, L. Gu, K. Lin, J. S. Miller, C. S. Chen, M. J. Sailor, S. N. Bhatia, *J. Am. Chem. Soc.* **2011**, *133*, 19582; b) R. Guillet-Nicolas, A. Popat, J. L. Bridot, G. Monteith, S. Z. Qiao, F. Kleitz, *Angew. Chem. Int. Ed.* **2013**, *52*, 2318; c) Y. Wang, M. S. Shim, N. S. Levinson, H. W. Sung, Y. Xia, *Adv. Funct. Mater.* **2014**, *24*, 4206; d) Y. Zhao, Z. Li, S. Kabehie, Y. Y. Botros, J. F. Stoddart, J. I. Zink, *J. Am. Chem. Soc.* **2010**, *132*, 13016.

[5] a) Y. Cui, H. Dong, X. Cai, D. Wang, Y. Li, *ACS Appl. Mater. Interfaces* **2012**, *4*, 3177; b) Z. Zheng, X. Huang, M. Schenderlein, D. Borisova, R. Cao, H. Mohwald, D. Shchukin, *Adv. Funct. Mater.* **2013**, *23*, 3307.

[6] a) W. Fang, J. Yang, J. Gong, N. Zheng, *Adv. Funct. Mater.* **2012**, *22*, 842; b) C. L. Zhu, C. H. Lu, X. Y. Song, H. H. Yang, X. R. Wang, *J. Am. Chem. Soc.* **2011**, *133*, 1278; c) C. Hom, J. Lu, M. Liong, H. Luo, Z. Li, J. I. Zink, F. Tamanoi, *Small* **2010**, *6*, 1185.

[7] a) S. Wu, X. Huang, X. Du, *Angew. Chem. Int. Ed.* **2013**, *52*, 5580; b) L. He, Y. Huang, H. Zhu, G. Pang, W. Zheng, Y. S. Wong, T. Chen, *Adv. Funct. Mater.* **2014**, *24*, 2754; c) G. Zhang, M. Yang, D. Cai, K. Zheng, X. Zhang, L. Wu, Z. Wu, *ACS Appl. Mater. Interfaces* **2014**, *6*, 8042.

[8] a) K. Patel, S. Angelos, W. R. Dichtel, A. Coskun, Y. W. Yang, J. I. Zink, J. F. Stoddart, *J. Am. Chem. Soc.* **2008**, *130*, 2382; b) C. Y. Lai, B. G. Trewyn, D. M. Jeftinija, K. Jeftinija, S. Xu, S. Jeftinija, V. S. Y. Lin, *J. Am. Chem. Soc.* **2003**, *125*, 4451; c) M. Bouchoucha, R. C. Gaudreault, M.-A. Fortin, F. Kleitz, *Adv. Funct. Mater.* **2014**, *24*, 5911.

[9] a) H. Lee, S. Kim, B. H. Choi, M. T. Park, J. Lee, S. Y. Jeong, E. K. Choi, B. U. Lim, C. Kim, H. J. Park, *Int. J. Hyperthermia* **2011**, *27*, 698; b) B. Chang, D. Chen, Y. Wang, Y. Chen, Y. Jiao, X. Sha, W. Yang, *Chem. Mater.* **2013**, *25*, 574.

[10] a) K. Knop, R. Hoogenboom, D. Fischer, U. S. Schubert, *Angew. Chem. Int. Ed.* **2010**, *49*, 6288; b) J. H. Ryu, S. Bickerton, J. Zhuang, S. Thayumanavan, *Biomacromolecules* **2012**, *13*, 1515; c) S. Jiwpanich, J. H. Ryu, S. Bickerton, S. Thayumanavan, *J. Am. Chem. Soc.* **2010**, *132*, 10683.

[11] a) K. Ock, W. I. Jeon, E. O. Ganbold, M. Kim, J. Park, J. H. Seo, K. Cho, S. W. Joo, S. Y. Lee, *Anal. Chem.* **2012**, *84*, 2172; b) F. Meng, R. Cheng, C. Deng, Z. Zhong, *Mater. Today* **2012**, *15*, 436; c) G. Adamo, N. Grimaldi, S. Campora, M. A. Sabatino, C. Dispenza, G. Ghers, *Chem. Eng. Trans.* **2013**, *38*, 457; d) D. C. González-Toro, J. H. Ryu, R. T. Chacko, J. Zhuang, S. Thayumanavan, *J. Am. Chem. Soc.* **2012**, *134*, 6964; e) X. Ma, O. S. Onga, Y. Zhao, *Biomater. Sci.* **2013**, *1*, 912.

[12] Q. Cai, Z. S. Luo, W. Q. Pang, Y. W. Fan, X. H. Chen, F. Z. Cui, *Chem. Mater.* **2001**, *13*, 258.

[13] a) J. Kim, H. Y. Nam, T. L. Kim, P. H. Kim, J. Ryu, C. O. Yun, S. W. Kim, *Biomaterials* **2011**, *32*, 5158; b) S. Chia, J. Cao, J. F. Stoddart, J. I. Zink, *Angew. Chem. Int. Ed.* **2001**, *40*, 2447; c) S. Saha, K. C. F. Leung, T. D. Nguyen, J. F. Stoddart, J. I. Zink, *Adv. Funct. Mater.* **2007**, *17*, 685; d) H. Kim, S. Kim, C. Park, H. Lee, H. J. Park, C. Kim, *Adv. Mater.* **2010**, *22*, 4280; e) Z. Chen, Z. Li, Y. Lin, M. Yin, J. Ren, X. Qu, *Chem. Eur. J.* **2013**, *19*, 1778; f) J. Lee, H. Kim, S. Kim, H. Lee, J. Kim, N. Kim, H. J. Park, E. K. Choi, J. S. Lee, C. Kim, *J. Mater. Chem* **2012**, *22*, 14061.

[14] a) A. D. Walkey, J. B. Olsen, H. Guo, A. Emili, W. C. W. Chan, *J. Am. Chem. Soc.* **2012**, *134*, 2139; b) R. K. Jai, T. Stylianopoulos, *Nat. Rev. Clin. Oncol.* **2010**, *2*, 653; c) A. Albanese, A. K. Lam, E. A. Sykes, J. V. Rocheleau, W. C. W. Chan, *Nat. Commun.* **2013**, *4*, 2718.

[15] a) Y. Lee, K. Miyata, M. Oba, T. Ishii, S. Fukushima, M. Han, H. Koyama, N. Nishiyama, K. Kataoka, *Angew. Chem. Int. Ed.* **2008**, *47*, 5163; b) A. S. Narang, D. Delmarre, D. Gao, *Int. J. Pharmaceutics* **2007**, *345*, 9; c) X. Zhao, Z. Poon, A. C. Engler, D. K. Bonner, P. T. Hammond, *Biomacromolecules* **2012**, *13*, 1315.

[16] J. H. Ryu, R. T. Chacko, S. Jiwpanich, S. Bickerton, R. P. Babu, S. Thayumanavan, *J. Am. Chem. Soc.* **2010**, *132*, 17227.

[17] a) A. Verma, F. Stellacci, *Small* **2010**, *6*, 12; b) S. E. A. Gratton, P. A. Ropp, P. D. Pohlhaus, J. C. Luft, V. J. Madden, M. E. Napier, J. M. DeSimone, *Proc. Natl. Acad. Sci. U.S.A.* **2008**, *33*, 11613; c) S. P. Victor, W. Paul, M. Jayabalan, C. P. Sharma, *Cryst. Eng. Commun.* **2014**, *16*, 6929; d) Z. G. Yue, W. Wei, P. P. Lv, H. Yue, L. Y. Wang, Z. G. Su, G. H. Ma, *Biomacromolecules* **2011**, *12*, 2440.

[18] a) J. Park, T. F. Brust, H. J. Lee, S. C. Lee, V. J. Watts, Y. Yeo, *ACS Nano* **2014**, *8*, 3347; b) J. Wu, C. Zhao, R. Hu, W. Lin, Q. Wang, J. Zhao, S. M. Bilinovich, T. C. Leeper, L. Li, H. M. Cheung, S. Chen, J. Zheng, *Acta Biomater.* **2014**, *10*, 751; c) A. Kolate, D. Baradia, S. Patil, I. Vhora, G. Kore, A. Misra, *J. Controlled Release* **2014**, *192*, 67.

[19] a) Q. Dai, C. Walkey, W. C. W. Chan, *Angew. Chem. Int. Ed.* **2014**, *53*, 5093; b) K. N. Yang, C. Q. Zhang, W. Wang, P. C. Wang, J. P. Zhou, X. J. Liang, *Cancer Biol. Med.* **2014**, *11*, 34.

[20] a) Q. Zhang, F. Liu, K. T. Nguyen, X. Ma, X. Wang, B. Xing, Y. Zhao, *Adv. Funct. Mater.* **2012**, *22*, 5144; b) X. Ma, K. T. Nguyen, P. Borah, C. Y. Ang, Y. Zhao, *Adv. Healthcare Mater.* **2012**, *1*, 690.

[21] K. Zhang, L. L. Xu, J. G. Jiang, N. Calin, K. F. Lam, S. J. Zhang, H. H. Wu, G. D. Wu, B. Albela, L. Bonneviot, P. Wu, *J. Am. Chem. Soc.* **2013**, *135*, 2427.

[22] a) K. Chen, X. Chen, *Theranostics* **2011**, *1*, 189; b) S. Balasubramanian, D. Kuppuswamy, *J. Biol. Chem.* **2003**, *278*, 42214.

[23] Z. Luo, X. Ding, Y. Hu, S. Wu, Y. Xiang, Y. Zeng, B. Zhang, H. Yan, H. Zhang, L. Zhu, J. Liu, J. Li, K. Cai, Y. Zhao, *ACS Nano* **2013**, *7*, 10271.

[24] a) N. Schleicha, P. Sibret, P. Danhier, B. Ucakar, S. Laurent, R. N. Muller, C. Jérôme, B. Gallezc, V. Préat, F. Danhier, *Int. J. Pharmaceutics* **2013**, *447*, 94; b) M. Das, S. K. Sahoo, *PLOS One* **2012**, *7*, e32920; c) K. Numata, S. Yamazaki, N. Naga, *Biomacromolecules* **2012**, *13*, 1383; d) W. Wang, Y. Wen, L. Xu, H. Du, Y. Zhou, X. Zhang, *Chem. Eur. J.* **2014**, *20*, 7796.

[25] a) G. S. Kwon, K. Kataoka, *Adv. Drug Delivery Rev.* **2012**, *64*, 237; b) S. Sengupta, D. Eavarone, I. Capila, G. L. Zhao, N. Watson, T. Kiziltepe, R. Sasisekharan, *Nature* **2005**, *436*, 568; c) N. Kolishetti, S. Dhar, P. M. Valencia, L. Q. Lin, R. Karnik, S. J. Lippard, R. Langer, O. C. Farokhzad, *Proc. Natl. Acad. Sci. U.S.A.* **2010**, *107*, 17939.

[26] a) L. D. Attardi, A. de Vries, T. Jacks, *Oncogene* **2004**, *23*, 973; b) D. L. Ma, C. M. Che, *Chem. Eur. J.* **2003**, *9*, 6133; c) S. Goto, Y. Ihara, Y. Urata, S. Izumi, K. Abe, T. Koji, T. Kondo, *FASEB. J.* **2001**, *15*, 2702.